Design of Digital Fractional Order Differentiator Using Discrete Sine Transform

Chien-Cheng Tseng* and Su-Ling Lee†
*Department of Computer and Communication Engineering, National Kaohsiung First University of Science and Technology, Kaohsiung, Taiwan, R.O.C.
E-mail: tcc@nkfust.edu.tw Tel: +886-7-6011000 ext 2029
†Department of Computer Science and Information Engineering, Chang-Jung Christian University, Tainan, Taiwan, R.O.C.
E-mail: lilee@mail.cjcu.edu.tw Tel: +886-6-2785123 ext 6155

***Abstract*— In this paper, the designs of digital fractional order differentiator (DFOD) using discrete sine transforms (DST) are presented. First, the definition of fractional differentiation is reviewed briefly. Then, the DST-based interpolation method is applied to compute the fractional differentiation of a given digital signal. Next, the transfer functions of DFOD are obtained from the DST computational results by using index mapping method. Finally, some numerical and application examples are demonstrated to show the effectiveness of the proposed DST-based design method.**

I. INTRODUCTION

In recent years, fractional order signal processing has received great attentions in many engineering applications. The research topics include fractional Fourier transform, fractional stochastic processes and fractional calculus [1]-[4]. In the research area of fractional calculus, the integer order n of derivative $D^n x(t)$ of function $x(t)$ is generalized to fractional order $D^\upsilon x(t)$, where υ is a real number. So far, fractional calculus have extensively used in the engineering applications including electromagnetic theory, automatic control, system identification, and biomedical applications [3][4]. Some typical applications of fractional calculus to digital signal processing are also described below: Firstly, fractional differential operator has been used to enhance the performance of linear prediction of speech signal [5]. Second is the signature verification where fractional differential operator is applied to extract the dynamic feature from the handwritten signature [6]. Third is the one-dimensional (1-D) and two-dimensional (2-D) linear-phase filter designs [7][8].

One of important research topics in fractional calculus is to implement the fractional operator D^υ in continuous and discrete time domains. For continuous time case, some methods for obtaining an approximated rational function using evaluation, interpolation and curve fitting techniques have been studied. These methods include Carlson's method, Roy's method, Chareff's method and Oustaloup's method [9]. For discrete time case, there have been several methods presented to design digital FIR and IIR fractional order differentiators for implementing operator D^υ including Taylor series expansion [10], continued fraction method [11], fractional sample-delay method [12], iterative method [13] and radial basis function method [14].

On the other hand, A.K. Jain has shown that for a first-order Markov sequence, with given boundary conditions, the Karhunen-Loeve transform, which is known to be statistically optimal, reduces to the discrete sine transform (DST) [15]. Until now, DST has been successfully applied to transform-domain adaptive filtering [16], signal interpolation [17], image coding and compression [18], speech enhancement [19], image encryption [20] and underwater target recognition and classification [21]. Moreover, there have been several fast computation algorithms proposed to compute the discrete sine transform including sparse-matrix factorization, fast recursive algorithm and prime factor decomposition etc [22]-[24]. Because the DST is highly computation-intensive, several dedicated architectures are also suggested for its implementation in very large-scale integration (VLSI) systems. The systolic array has the advantages of pipelinability, regularity, locality and scalability, so various systolic arrays for DST and its inverse have been developed in the literature [25][26].

In this paper, we will use DST-based interpolation method and Grünwald-Letnikov fractional differentiation to design digital fractional order differentiator. This paper is organized as follows. In section II, the definitions of fractional differentiation are reviewed briefly. In section III, the type I DST is applied to design digital fractional order differentiator. Because the closed-form design is obtained, the filter coefficients are easily computed without performing any optimization. In section IV, the design results of other three types of DST's are presented. In section V, the comparisons, discussions, and application examples are presented. Finally, a conclusion is made.

II. FRACTIONAL DIFFERENTIATION

In the literature, there are several definitions of fractional differentiation and integral such as Riemann-Liouville and Grünwald-Letnikov [1]-[4]. In this paper, we will use the Grünwald-Letnikov differentiation whose definition is

$$D^\upsilon f(x) = \frac{d^\upsilon f(x)}{dx^\upsilon} = \lim_{\Delta \to 0} \sum_{k=0}^{\infty} \frac{(-1)^k C_k^\upsilon}{\Delta^\upsilon} f(x - k\Delta) \tag{1}$$

where coefficient C_k^{υ} is given by

$$C_k^{\upsilon} = \frac{\Gamma(\upsilon+1)}{\Gamma(k+1)\Gamma(\upsilon-k+1)} = \begin{cases} 1 & k=0 \\ \dfrac{\upsilon(\upsilon-1)(\upsilon-2)\cdots(\upsilon-k+1)}{1.2.3\cdots k} & k \geq 1 \end{cases} \quad (2)$$

The above notation $\Gamma(\cdot)$ is the gamma function. Based on this definition, it can be shown that the fractional differentiations of exponential, power and trigonometric functions are given by

$$D^{\upsilon} e^{\alpha x} = \alpha^{\upsilon} e^{\alpha x} \quad (3a)$$

$$D^{\upsilon} x^{q} = \frac{\Gamma(q+1)}{\Gamma(q-\upsilon+1)} x^{q-\upsilon} \quad (3b)$$

$$D^{\upsilon} A\sin(\omega x+\phi) = A\omega^{\upsilon}\sin(\omega x+\phi+\tfrac{\pi}{2}\upsilon) \quad (3c)$$

$$D^{\upsilon} A\cos(\omega x+\phi) = A\omega^{\upsilon}\cos(\omega x+\phi+\tfrac{\pi}{2}\upsilon) \quad (3d)$$

So far, the definition of fractional differentiation has described. In next sections, we will use the Grünwald-Letnikov differentiation in (1) and discrete sine transform to design digital fractional order differentiator.

III. Design Method Using DST-I

In the literature, there are four types of discrete sine transforms, namely DST-I, DST-II, DST-III and DST-IV [27]. In this section, the DST-I design method is presented. Given the discrete-time sequence $x(0)$, $x(1)$, ..., $x(N-1)$ which are sampled from continuous-time signal $x(t)$, let us first study how to compute the fractional differentiation $D^{\upsilon}x(t)$ using DST-I. The DST-I is defined as

$$X(k) = \sqrt{\frac{2}{N+1}}\sum_{n=0}^{N-1} x(n)\sin(\tfrac{(n+1)(k+1)\pi}{N+1}) \quad (4a)$$

$$x(n) = \sqrt{\frac{2}{N+1}}\sum_{k=0}^{N-1} X(k)\sin(\tfrac{(n+1)(k+1)\pi}{N+1}) \quad (4b)$$

Substituting forward DST-I in (4a) into inverse DST-I in (4b), we get

$$x(n) = \sqrt{\frac{2}{N+1}}\sum_{k=0}^{N-1}\left(\sqrt{\frac{2}{N+1}}\sum_{m=0}^{N-1} x(m)\sin(\tfrac{(m+1)(k+1)\pi}{N+1})\right)\sin(\tfrac{(n+1)(k+1)\pi}{N+1}) \quad (5)$$

$$= \sum_{m=0}^{N-1} x(m)\left\{\frac{2}{N+1}\sum_{k=0}^{N-1}\sin\left(\tfrac{(m+1)(k+1)\pi}{N+1}\right)\sin\left(\tfrac{(n+1)(k+1)\pi}{N+1}\right)\right\}$$

Replacing discrete-time variable n by continuous-time variable t, the interpolated signal $x(t)$ is given by

$$x(t) = \sum_{m=0}^{N-1} x(m)b(m,t) \quad (6)$$

where the interpolation basis is given by

$$b(m,t) = \frac{2}{N+1}\sum_{k=0}^{N-1}\sin\left(\tfrac{(m+1)(k+1)\pi}{N+1}\right)\sin\left(\tfrac{(t+1)(k+1)\pi}{N+1}\right) \quad (7)$$

Taking the υ-th order fractional differentiation at both sides of equation (6), it yields

$$D^{\upsilon}x(t) = \sum_{m=0}^{N-1} x(m)[D^{\upsilon}b(m,t)] \quad (8)$$

Using linear property of fractional differentiation and the (3c)(7), we have

$$D^{\upsilon}b(m,t) = \frac{2}{N+1}\sum_{k=0}^{N-1}\left(\frac{(k+1)\pi}{N+1}\right)^{\upsilon}\sin\left(\tfrac{(m+1)(k+1)\pi}{N+1}\right)\sin\left(\tfrac{(t+1)(k+1)\pi}{N+1}+\tfrac{\pi}{2}\upsilon\right) \quad (9)$$

Substituting (9) into (8), we get fractional differentiation of signal $x(t)$ below:

$$D^{\upsilon}x(t) = \sum_{m=0}^{N-1} x(m)p_m(t) \quad (10)$$

with

$$p_m(t) = \frac{2}{N+1}\sum_{k=0}^{N-1}\left(\frac{(k+1)\pi}{N+1}\right)^{\upsilon}\sin\left(\tfrac{(m+1)(k+1)\pi}{N+1}\right)\sin\left(\tfrac{(t+1)(k+1)\pi}{N+1}+\tfrac{\pi}{2}\upsilon\right) \quad (11)$$

In what follows, let us use the result in (10) to obtain the transfer function of digital fractional order differentiator whose frequency response approximates the following ideal response well:

$$H_d(\omega) = (j\omega)^{\upsilon}e^{-j\omega I} \quad (12)$$

where I is a prescribed delay. The transfer function of FIR filter is given by

$$H(z) = \sum_{r=0}^{N-1} h(r)z^{-r} \quad (13)$$

When a signal $s(n)$ passes through this FIR filter, its output is the weighted average of the integer delayed samples $s(n)$, $s(n-1)$, $s(n-2)$,..., $s(n-N+1)$, that is, the output is

$$y(n) = \sum_{r=0}^{N-1} h(r)s(n-r) \quad (14)$$

Now, the problem is how to use the formula in (10) to determine filter coefficients $h(r)$ such that the filter output $y(n)$ is almost equal to the delayed fractional differentiation $D^{\upsilon}s(n-I)$, that is,

$$y(n) \approx D^{\upsilon}s(n-I) \quad (15)$$

In the following, an index mapping method is used to solve this problem. If we choose

$$\begin{aligned} s(n) &= x(N-1) \\ s(n-1) &= x(N-2) \\ &\vdots \\ s(n-N+1) &= x(0) \end{aligned} \quad (16)$$

then equations (10) and (14) can be linked together. Equation (16) can be rewritten as the form

$$x(m) = s(n-(N-1)+m) \qquad 0 \leq m \leq N-1 \quad (17)$$

Substituting (17) and $x(t) = s(n-(N-1)+t)$ into equation (10), we get

$$D^{\upsilon}s(n-(N-1)+t)=\sum_{m=0}^{N-1}s(n-(N-1)-m)p_m(t) \qquad (18)$$

Let $r=(N-1)-m$, the expression becomes

$$D^{\upsilon}s(n-(N-1)+t)=\sum_{r=0}^{N-1}s(n-r)p_{N-1-r}(t) \qquad (19)$$

Moreover, let $I=(N-1)-t$, equation (19) reduces to

$$D^{\upsilon}s(n-I)=\sum_{r=0}^{N-1}s(n-r)p_{N-1-r}(N-1-I) \qquad (20)$$

Compared (14) with (20), it can be found that if we choose

$$h(r)=p_{N-1-r}(N-1-I) \qquad (21)$$

then it yields

$$D^{\upsilon}s(n-I)=\sum_{r=0}^{N-1}h(r)s(n-r) \qquad (22)$$

that is, equation (15) is valid . Substituting (11) into (21), the filter coefficients are given by

$$h(r)=\frac{2}{N+1}\sum_{k=0}^{N-1}\left(\frac{(k+1)\pi}{N+1}\right)^{\upsilon}\sin\left(\frac{(N-r)(k+1)\pi}{N+1}\right)\sin\left(\frac{(N-I)(k+1)\pi}{N+1}+\frac{\pi}{2}\upsilon\right) \qquad (23)$$

Finally, two remarks are made. First, the closed-form design in (23) is obtained, so the filter coefficients are easily computed without performing any optimization. Second, filter coefficients can be modified by the Hamming window

$$w(r)=0.54-0.46\cos\left(\frac{2\pi r}{N-1}\right) \qquad (24)$$

to get the window-based design, that is, the modified filter coefficients are given by

$$h_w(r)=h(r)w(r) \qquad (25)$$

Now, two examples are used to show the effectiveness of the proposed DST-I digital fractional order differentiators. To evaluate the performance, the integral squares error of frequency response is defined by

$$E=\sqrt{\int_0^{\lambda\pi}\left|H(e^{j\omega})-H_d(\omega)\right|^2 d\omega} \qquad (26)$$

Obviously, the smaller the error E is, the better performance of design method has.

Example 1: In this example, we will study the relation between design error E and delay I in the DST-I case. The design parameters are chosen as $N=80$, $\upsilon=0.2$ and $\lambda=0.9$. Fig.1 shows the error curve E of the proposed DST-I based fractional order differentiator $H(z)$ for the non-windowed design in (23) and windowed design in (25). The parameter I ranges from 30 to 50. From these results, it can be seen that the errors of windowed design reach the minimum value when $I\approx N/2$ is chosen. And, the errors of non-windowed design are almost equal to a constant for all delay values I. Moreover, the non-windowed design has smaller errors than the windowed design in this case.

Example 2: In this example, let us study the relation between design error E and fractional order υ in the DST-I case. The design parameters are chosen as $N=80$, $I=40$ and $\lambda=0.9$. Fig.2 shows the error curve E of the proposed DST-I based fractional order differentiator $H(z)$ for the non-windowed and windowed designs. The parameter υ ranges from 0.1 to 1. From these results, it can be seen that the non-windowed design has smaller errors than the windowed design for orders υ in [0.1,0.8]. Moreover, Fig.3(a) shows the magnitude responses (solid line) of the differentiator $H(z)$ of the windowed design with $I=40$ and $\upsilon=0.5$. The dashed line is the ideal magnitude response ω^{υ}. So, the specification is fitted well except the region near $\omega=\pi$. Fig.3(b) depicts the normalized phase response $90*[angle(H(e^{j\omega}))+\omega I]/0.5\pi$ in degree. The dashed line is the ideal response 90υ. It can be observed that the specification is well approximated except the region near $\omega=0$ and $\omega=\pi$.

So far, the design method and design results of type I discrete sine transform have been described. In next section, the design results of the other three types of discrete sine transforms will be studied and reported.

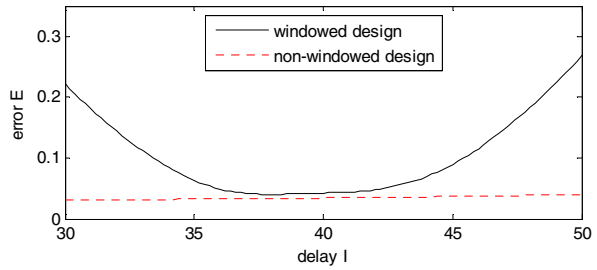

Fig.1 The error curve E of the proposed DST-I based fractional order differentiator $H(z)$ for delay values I.

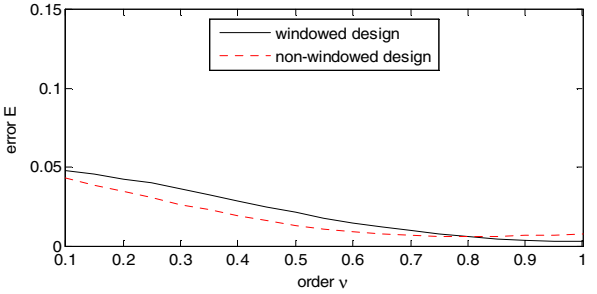

Fig.2 The error curve E of the proposed DST-I based fractional order differentiator $H(z)$ for orders υ.

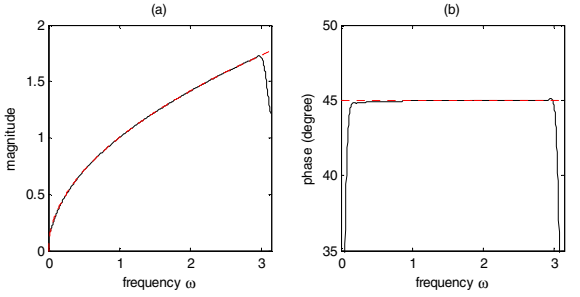

Fig.3 The designed results (solid line) of the windowed DST-I based digital fractional order differentiator $H(z)$ for $\upsilon=0.5$. (a) Magnitude response. (b) Phase response. The dashed line is the ideal response.

IV. DESIGN METHODS USING OTHER TYPES OF DST

In this section, design methods of other three types of discrete sine transforms are studied including type II DST (DST-II), type III DST (DST-III) and type IV DST (DST-IV). The numerical examples of these methods are also illustrated.

A. Design Method Based on DST-II

The type II discrete sine transform is defined as

$$X(k) = \sqrt{\frac{2}{N}} \sum_{n=0}^{N-1} c_k x(n) \sin\left(\frac{(n+0.5)(k+1)\pi}{N}\right) \quad (27a)$$

$$x(n) = \sqrt{\frac{2}{N}} \sum_{k=0}^{N-1} c_k X(k) \sin\left(\frac{(n+0.5)(k+1)\pi}{N}\right) \quad (27b)$$

where

$$c_k = \begin{cases} \frac{1}{\sqrt{2}} & k = N-1 \\ 1 & otherwise \end{cases} \quad (28)$$

Using the similar method in DST-I, it can be deduced that the filter coefficients of DST-II based digital fractional order differentiator are given by

$$h(r) = \frac{2}{N} \sum_{k=0}^{N-1} c_k^2 \left(\frac{(k+1)\pi}{N}\right)^{\upsilon} \sin\left(\frac{(N-r-0.5)(k+1)\pi}{N}\right) \sin\left(\frac{(N-I-0.5)(k+1)\pi}{N} + \frac{\pi}{2}\upsilon\right) \quad (29)$$

For windowed design, the modified filter coefficients are also given by $h_w(r) = h(r)w(r)$. Now, two examples are used to show the effectiveness of the proposed DST-II digital fractional order differentiators.

Example 3: In this example, we will study the relation between design error E and delay I in the DST-II case. The design parameters are chosen as $N = 80$, $\upsilon = 0.2$ and $\lambda = 0.9$. Fig.4 shows the error curve E of the proposed DST-II based fractional order differentiator $H(z)$ for the non-windowed design in (29) and its windowed design. From these results, it can be seen that the errors of windowed design reach the minimum value when $I \approx N/2$ is chosen. And, the errors of non-windowed design are almost equal to a constant for all delay values I, but there is an oscillating behavior in the error curve of E.

Example 4: In this example, let us study the relation between design error E and fractional order υ in the DST-II case. The design parameters are chosen as $N = 80$, $I = 40$ and $\lambda = 0.9$. Fig.5 shows the error curve E of the proposed DST-II based fractional order differentiator $H(z)$ for the non-windowed and windowed designs. From these results, it can be seen that the windowed design has smaller errors than the non-windowed design for orders υ in [0.35,1]. Moreover, Fig.6(a) shows the magnitude responses of the differentiator $H(z)$ of the windowed design with $I = 40$ and $\upsilon = 0.5$. So, the specification is fitted well except the region near $\omega = \pi$. Fig.6(b) depicts the normalized phase response. It can be observed that the specification is well approximated except the region near $\omega = 0$ and $\omega = \pi$.

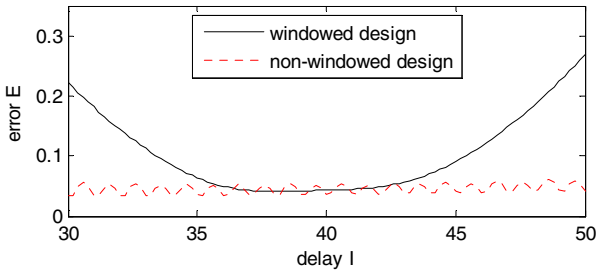

Fig.4 The error curve E of the proposed DST-II based fractional order differentiator $H(z)$ for delay values I.

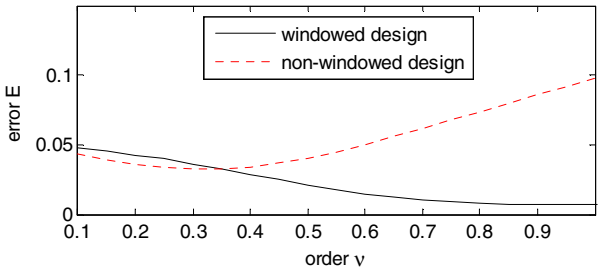

Fig.5 The error curve E of the proposed DST-II based fractional order differentiator $H(z)$ for orders υ.

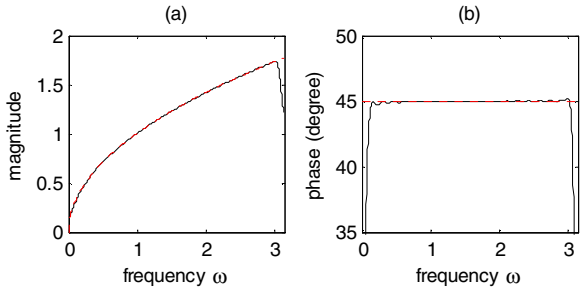

Fig.6 The designed results (solid line) of the windowed DST-II based digital fractional order differentiator $H(z)$ for $\upsilon = 0.5$. (a) Magnitude response. (b) Phase response. The dashed line is the ideal response.

B. Design Method Based on DST-III

The type III discrete sine transform is defined as

$$X(k) = \sqrt{\frac{2}{N}} \sum_{n=0}^{N-1} c_n x(n) \sin\left(\frac{(n+1)(k+0.5)\pi}{N}\right) \quad (30a)$$

$$x(n) = \sqrt{\frac{2}{N}} \sum_{k=0}^{N-1} c_n X(k) \sin\left(\frac{(n+1)(k+0.5)\pi}{N}\right) \quad (30b)$$

where

$$c_n = \begin{cases} \frac{1}{\sqrt{2}} & n = N-1 \\ 1 & otherwise \end{cases} \quad (31)$$

Using the similar method in DST-I, it can be deduced that the filter coefficients of DST-III based digital fractional order differentiator are given by

$$h(r)=\frac{2}{N}\sum_{k=0}^{N-1}c_{N-1-r}c_{N-1-l}\left(\frac{(k+0.5)\pi}{N}\right)^{\upsilon}\sin\left(\frac{(N-r)(k+0.5)\pi}{N}\right)\sin\left(\frac{(N-l)(k+0.5)\pi}{N}+\frac{\pi}{2}\upsilon\right) \tag{32}$$

For windowed design, the modified filter coefficients are given by $h_w(r)=h(r)w(r)$. Now, two examples are used to show the effectiveness of the proposed DST-III digital fractional order differentiators.

Example 5: In this example, we will study the relation between design error E and delay I in the DST-III case. The parameters are chosen as $N=80$, $\upsilon=0.2$ and $\lambda=0.9$. Fig.7 shows the error curve E of the proposed DST-III based fractional order differentiator $H(z)$ for the non-windowed design in (32) and its windowed design. From these results, it can be seen that the errors of windowed design also reach the minimum value when $I\approx N/2$ is chosen.

Example 6: In this example, let us study the relation between design error E and fractional order υ in the DST-III case. The parameters are chosen as $N=80$, $I=40$ and $\lambda=0.9$. Fig.8 shows the error curve E of the proposed DST-III based fractional order differentiator $H(z)$ for the non-windowed and windowed designs. From these results, it can be seen that the windowed design has smaller errors than the non-windowed design for orders υ in [0.35,1]. Moreover, Fig.9(a) shows the magnitude responses of the differentiator $H(z)$ of the windowed design with $I=40$ and $\upsilon=0.5$. So, the specification is fitted well except the region near $\omega=\pi$. Fig.9(b) depicts the normalized phase response. It can be observed that the specification is well approximated except the region near $\omega=0$ and $\omega=\pi$.

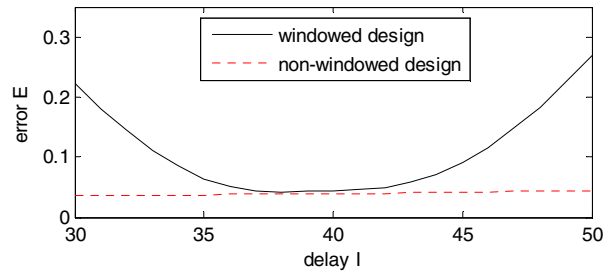

Fig.7 The error curve E of the proposed DST-III based fractional order differentiator $H(z)$ for delay values I.

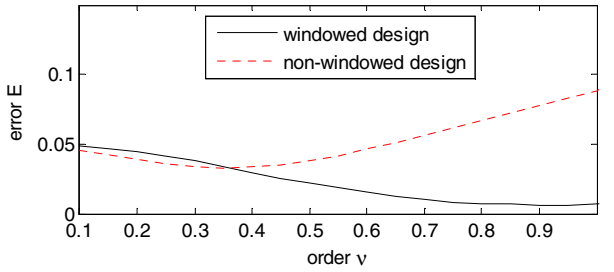

Fig.8 The error curve E of the proposed DST-III based fractional order differentiator $H(z)$ for orders υ.

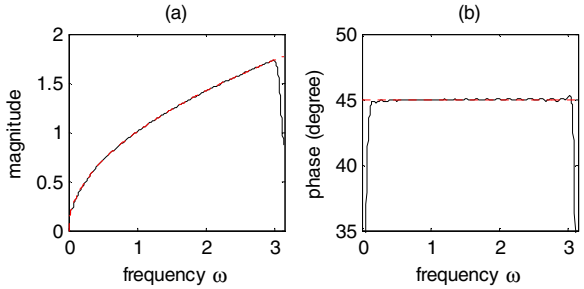

Fig.9 The designed results (solid line) of the windowed DST-III based digital fractional order differentiator $H(z)$ for $\upsilon=0.5$. (a) Magnitude response. (b) Phase response. The dashed line is the ideal response.

C. Design Method Based on DST-IV

The type IV discrete sine transform is defined as

$$X(k)=\sqrt{\frac{2}{N}}\sum_{n=0}^{N-1}x(n)\sin\left(\frac{(n+0.5)(k+0.5)\pi}{N}\right) \tag{33a}$$

$$x(n)=\sqrt{\frac{2}{N}}\sum_{k=0}^{N-1}X(k)\sin\left(\frac{(n+0.5)(k+0.5)\pi}{N}\right) \tag{33b}$$

Using the similar method in DST-I, it can be deduced that the filter coefficients of DST-IV based digital fractional order differentiator are given by

$$h(r)=\frac{2}{N}\sum_{k=0}^{N-1}\left(\frac{(k+0.5)\pi}{N}\right)^{\upsilon}\sin\left(\frac{(N-r-0.5)(k+0.5)\pi}{N}\right)\sin\left(\frac{(N-l-0.5)(k+0.5)\pi}{N}+\frac{\pi}{2}\upsilon\right) \tag{34}$$

For windowed design, the modified filter coefficients are given by $h_w(r)=h(r)w(r)$. Now, two numerical examples are used to show the effectiveness of the proposed DST-IV digital fractional order differentiators.

Example 7: In this example, we will study the relation between design error E and delay I in the DST-IV case. The design parameters are chosen as $N=80$, $\upsilon=0.2$ and $\lambda=0.9$. Fig.10 shows the error curve E of the proposed DST-II based fractional order differentiator $H(z)$ for the non-windowed design in (34) and its windowed design. From these results, it can be seen that the errors of windowed design have the minimum value when $I\approx N/2$ is chosen.

Example 8: In this example, let us study the relation between design error E and fractional order υ in the DST-IV case. The design parameters are chosen as $N=80$, $I=40$ and $\lambda=0.9$. Fig.11 shows the error curve E of the proposed DST-IV based fractional order differentiator. From these results, it can be seen that the windowed design has smaller errors than the non-windowed design for orders υ in [0.35,1]. Moreover, Fig.12(a) shows the magnitude responses of the differentiator $H(z)$ of the windowed design with $I=40$ and $\upsilon=0.5$. So, the specification is fitted well except the region near $\omega=\pi$. Fig.12(b) depicts the normalized phase response. It can be observed that the specification is approximated well.

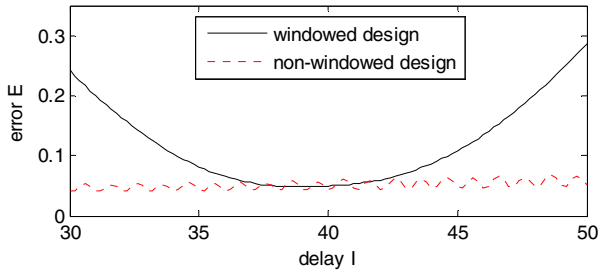

Fig.10 The error curve E of the proposed DST-IV based fractional order differentiator $H(z)$ for delay values I.

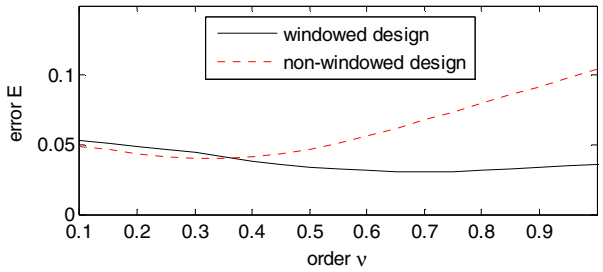

Fig.11 The error curve E of the proposed DST-IV based fractional order differentiator $H(z)$ for orders υ.

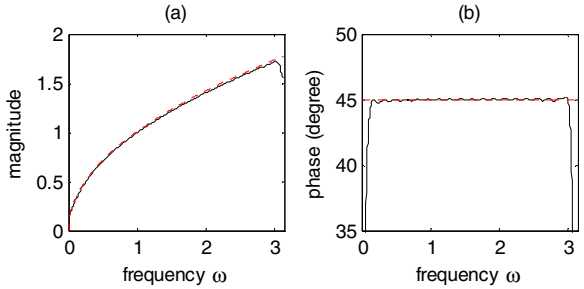

Fig.12 The designed results of the windowed DST-IV based digital fractional order differentiator $H(z)$ for $\upsilon = 0.5$. (a) Magnitude response. (b) Phase response. The dashed line is the ideal response.

Finally, let us compare the performances of four types of DST designs. After comparing the error curves E in Fig. 2, Fig5, Fig.8 and Fig.11, it is clear that the DST-I provides smaller design errors than those of DST-II, DST-III and DST-IV. Thus, the DST-I is the best choice if the DST is used to design digital fractional order differentiators.

V. Comparison, Discussion and Application

In this section, the performance comparisons, discussions and applications of the proposed DST-based digital fractional order differentiators will be presented.

A. Comparison with Conventional Method

Here, let us compare the proposed DST-I method with the conventional radial basis function (RBF) method in [14]. When the design parameters are chosen as $N = 100$, $I = 50$ and $\upsilon = 0.5$, Fig.13(a)(b) show the designed results (solid line) of the RBF method. The dashed line is the ideal response. Fig.13(c)(d) show the magnitude and phase responses (solid line) of the designed digital fractional order FIR differentiator using windowed DST-I method. The dashed line is the ideal response. Clearly, the phase response of the DST-I method is much better than the phase response of the RBF method. If $\lambda = 0.9$ is chosen, the error E of conventional RBF method in [14] is 0.0356, and the error E of proposed DST-I method is 0.0169. Thus, the proposed DST-I method has a smaller design error than the conventional RBF method in [14].

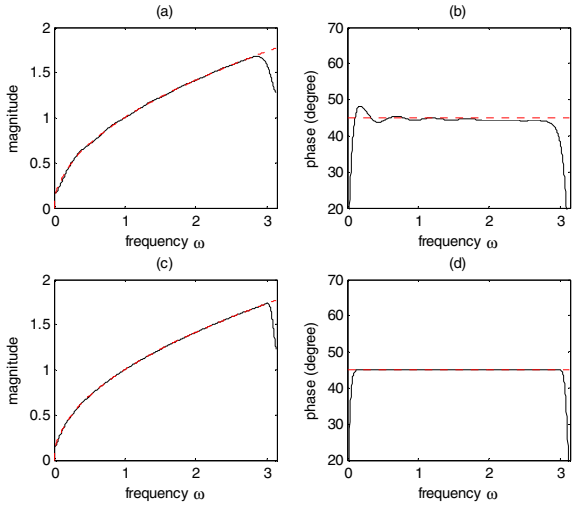

Fig.13 The designed results (solid line) of the fractional order FIR differentiator $H(z)$ for $\upsilon = 0.5$. (a)(b) The results of the RBF method in [14]. (c)(d) The results of the proposed DST-I method. The dashed line is the ideal response.

B. Discussion

Now, let us show how to use the DST-I method and the Prony method to design an IIR digital fractional order differentiator. If N is large, the designed fractional order differentiator is a long-length FIR filter. To reduce implementation complexity, the long-length FIR filter $H(z)$ can be approximated by an IIR filter below:

$$\hat{H}(z) = \frac{\sum_{n=0}^{N_1} h_1(n) z^{-n}}{1 + \sum_{n=1}^{N_1} h_2(n) z^{-n}} \qquad (35)$$

where filter coefficients $h_1(n)$ and $h_2(n)$ can be determined by the Prony method in [28]. Now, one example is illustrated below. The parameters are chosen as $N = 80$, $I = 18$, $N_1 = 20$, and $\upsilon = 0.5$. Fig.14(a)(b) show the magnitude and phase responses (solid line) of the designed IIR differentiator $\hat{H}(z)$ in (35). The dashed line is the ideal response. Clearly, the specification is fitted well except the region near $\omega = 0$ and $\omega = \pi$. The maximum pole radius is 0.947, so the IIR filter $\hat{H}(z)$ is stable.

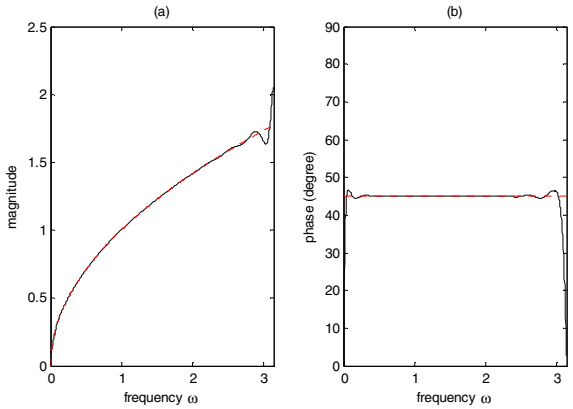

Fig.14 The designed results (solid line) of the DST-I based IIR digital fractional order differentiator $\hat{H}(z)$ for $\upsilon = 0.5$. (a) Magnitude response. (b) Phase response. The dashed line is the ideal response.

C. Application

In [29], we use the fractional derivative and Mach band effect to construct a color image sharpening method. This method is based on the one-dimensional (1-D) signal sharpening approach depicted in Fig.15, where the $H(z)$ is the transfer function of digital fractional order differentiator (DFOD). In [29], the DFOD $H(z)$ is designed by using fractional differencing approach. In this paper, the DFOD $H(z)$ is designed by discrete sine transform. Thus, it is interesting to compare their performances of both DFOD in the image sharpening application. Now, one example is illustrated. The scenario of experiment is exactly the same as the one in [29] except the $H(z)$ is designed by non-windowed DST-I method with parameters $N = 5$ and $I = 0.5$. The color space used here is the RGB space. Fig.16(a) shows the original image. Fig.16(b)(c) show the sharpened images by the method in [29] and DST method in this paper with fractional order $\upsilon = 0.5$. For comparison, the sharpened result of the Laplician method in [30] is also shown in Fig.16(d). From these results, it is clear that the sharpened image qualities of three methods look compatible by human eyes.

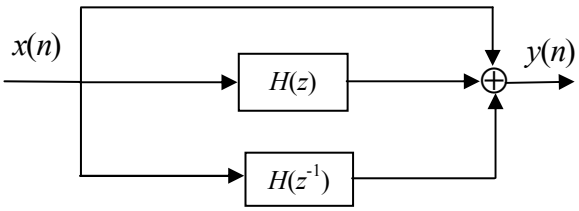

Fig.15 The block diagram using two digital fractional order differentiators $H(z)$ and $H(z^{-1})$ to sharpen the one dimensional (1-D) signal $x(n)$.

Fig.16(a)

Fig.16(b)

Fig.16(c)

Fig.16(d)

Fig.16 The results of the color image sharpening. (a) Original image. (b) The proposed DST-I method. (c) The method in [29]. (d) The Laplacian method in [30].

VI. Conclusions

In this paper, the designs of digital fractional order differentiators using four types of discrete sine transforms have been presented. First, the definition of fractional differentiation is reviewed briefly. Then, the DST-based interpolation method is applied to compute the fractional differentiation of a given digital signal. Next, the closed-form transfer functions of DFOD are obtained from the DST computational results by using index mapping method. Finally, some numerical and application examples are demonstrated to show the effectiveness of the proposed DST-based design method. However, only one dimensional DFOD is studied in this paper. Thus, it is interesting to study the two dimensional DFOD design using DST in the future.

References

[1] S. Das and I. Pan, *Fractional Order Signal Processing: Introductory Concepts and Applications*, Springer, 2012.

[2] H. Sheng, Y.Q. Chen and T.S. Qiu, *Fractional Processes and Fractional-Order Signal Processing: Techniques and Applications*, Springer, 2012.

[3] R. Herrmann, *Fractional Calculus: An Introduction for Physicists*, World Scientific, 2011.

[4] M.D. Ortigueira, *Fractional Calculus for Scientists and Engineers*, Springer, 2011.

[5] K. Assaleh, W.M. Ahmad, "Modeling of speech signals using fractional calculus," *in Proceedings of the 9th International Symposium on Signal Processing and Its Applications*, Feb. 2007.

[6] C.C. Tseng, "Design of variable and adaptive fractional order differentiators," *Signal Processing*, vol.86, pp.2554-2566, Oct. 2006.

[7] C.C. Tseng and S.L. Lee, "Design of linear phase FIR filters using fractional derivative constraints," *Signal Processing*, vol.92, pp.1317-1327, May 2012.

[8] C.C. Tseng and S.L. Lee, "Designs of two-dimensional linear phase FIR filters using fractional derivative constraints," *Signal Processing*, vol.93, pp.1141-1151, May 2013.

[9] A. Oustaloup, F. Levron, B. Mathieu and F.M. Nanot, "Frequency-band complex noninteger differentiator: characterization and synthesis," *IEEE Trans. on Circuits and Systems-I: Regular Papers,* vol.47, pp.25-39, Jan. 2000.

[10] C.C. Tseng, "Design of fractional order digital FIR differentiators," *IEEE Signal Processing Letters*, vol.8, pp.77-79, Mar. 2001.

[11] Y.Q. Chen and B.M. Vinagre, "A new IIR-type digital fractional order differentiator," *Signal Processing*, vol.83, pp.2359-2365, Oct. 2003.

[12] C.C. Tseng, "Improved design of digital fractional-order differentiators using fractional sample delay," *IEEE Trans. on Circuits and Systems-I: Regular Papers,* vol.53, pp.193-203, Jan. 2006.

[13] J.J. Shyu, S.C. Pei and C.H. Chan, "An iterative method for the design of variable fractional order FIR differintegrators," *Signal Processing*, vol.89, pp.320-327, Mar. 2009.

[14] C.C. Tseng and S.L. Lee, "Design of fractional order digital differentiator using radial basis function," *IEEE Trans. on Circuits and Systems-I: Regular Papers,* vol.57, pp.1708-1718, July 2010.

[15] A.K. Jain, "A fast Karhunen-Loeve transform for a class of random processes," *IEEE Trans. on Communications*, pp.1023-1029, Sept. 1976.

[16] J.C. Lee and C.K. Un, "Performance of transform-domain LMS adaptive digital filters," *IEEE Trans. on Acoustics, Speech, and Signal Processing*, pp.499-510, June 1986.

[17] Z. Wang, G.A. Jullien and W.C. Miller, "Interpolation using the discrete sine transform with increased accuracy," *Electronics Letters*, pp.1918-1920, Oct. 1993.

[18] E.G. Pelaes and Y. Iano, "Image coding using discrete sine transform with axis rotation," *IEEE Trans. on Consumer Electronics*, pp.1284-1290, Nov. 1998.

[19] X. Li, H. Xie and B. Cheng, "Noisy speech enhancement based on discrete sine transform," *in Proceedings of the 1st International Multi-Symposium on Computer and Computational Sciences*, 2006.

[20] H. Zhao, Q. Ran, G. Ge, J. Ma and L. Tan, "Image encryption based on random fractional discrete cosine and sine transforms," *in Proceedings of the 1st International Workshop on Education Technology and Computer Science*, pp.804-808. 2009.

[21] T. Binesh, M.H. Supriya and P.R.S. Pillai, "Discrete sine transform based HMM underwater signal classifier," *in Proceedings of International Symposium on Ocean Electronics*, pp.152-156, 2011.

[22] P. Yip and K.R. Rao, "A fast computational algorithm for the discrete sine transform," *IEEE Trans. on Communications*, pp.304-307, Feb. 1980.

[23] A. Gupta and K.R. Rao, "A fast recursive algorithm for the discrete sine transform," *IEEE Trans. on Acoustics, Speech, and Signal Processing*, pp.553-557, March 1990.

[24] D.C. Kar and V.V.B. Rao, "On the prime factor decomposition algorithm for the discrete sine transform," *IEEE Trans. on Signal Processing*, pp.3258-3260, Nov. 1994.

[25] L.W. Chang and M.C. Wu, "A unified systolic array for discrete cosine and sine transforms," *IEEE Trans. on Signal Processing*, pp.192-194, Jan. 1991.

[26] P.K. Meher and M.N.S. Swamy, "New systolic algorithm and array architecture for prime-length discrete sine transform," *IEEE Trans. on Circuits and Systems-II: Express Briefs*, pp.262-266, Mar. 2007.
[27] B. Porat, *A Course in Digital Signal Processing*, John Wiley & Sons, INC. 1997.
[28] L.B. Jackson, Digital Filters and Signal Processing, 3rd Edition, Boston, MA:Kluwer Academic, 1996.
[29] C.C. Tseng and S.L. Lee, "Digital image sharpening using fractional derivative and Mach band effect," *in Proceedings of IEEE International Symposium on Circuits and Systems*, pp.3174-3177, May 2012.
[30] R.C. Gonzalez and R.E. Woods, *Digital Image Processing*, Third Edition, Prentice-Hall, 2008.